Nat. Volatiles & Essent. Oils, 2021; 8(5): 1757 - 1766

NVEO
Natural Volatiles &
Essential Oils

Time-optimality of robots by minimizing the motion times in terms of spin, circular arc, and tangential motion

[1]Dr. Anandakumar Haldorai, [2]M. Arulaalan, [3] Mr. T.Thomas Leonid, [4]P. Suresh, [5]Dr. S. Markkandan, [6]Dr.Ram Subbiah

1 Professor (Associate), Department of Computer science and engineering, Sri Eshwar College of Engineering, Coimbatore, Tamil Nadu, India. 641202 anandakumar.psgtech@gmail.com
2 Professor & Head, Department of ECE, C K College of Engineering and Technology, Cuddalore. ecehod@ckcet.com
3 Assistant Professor, Sel Grade, ECE Department, KCG College of Technology. thomasleonid@kcgcollege.com
4 Dept of ECE, Veltech Rangarajan Dr Sagunthala R and D Institute of Science and Technology, Chennai, Tamilnadu, India. suresh3982@yahoo.co.in
5 Department of ECE, SRM TRP Engineering College, Trichy, Tamilnadu. India markkandan.s@trp.srmtrichy.edu.in
6 Associate Professor, Mechanical engineering, Gokaraju Rangaraju institute of Engineering and Technology, Hyderabad. ram4msrm@gmail.com

Abstract

In this paper, three omniwheels are positioned at an equilateral triangle having the vertices with wheel axles connected from the center of the triangle with the rays to every individual wheel in a typical mobile robot configuration. Omniwheels as normal wheels are moving perpendicularly to the direction of the wheel axle by the motors, however, unlike normal wheels, they may slide parallelly to the axle direction. Apart from a directed automobile, a time-optimal robot with such architecture may travel in either direction without rotating initially, and that can spin while doing so. Straight lines seem to be the shortest pathways for this time-optimal robot with minimum motion timing. The robot, on the other hand, might drive faster in certain various directions with minimum motion time. In this paper, we use a robot kinematic model to set independent speed boundaries with minimum motion time for the wheel and calculate the quickest analytical paths between setups. In this paper, the robot with minimum motion timing is analyzed in terms of spins, circular arcs, as well as a tangential motion to the wheel axles, which appear in the time-optimal trajectories of the robot. Thus, the sequence of various segments in time-optimal robot trajectories is analyzed.

Index Key: Time-optimal robot, Spin, Circular arc, Tangential motion, Switching function.

1. Introduction

Classical motion-planning issues addressed how an object is moving from a specified beginning point to the desired target point without striking anything. It might be known as the Object Mover's issue. Other components of the issue, including differential constraints, uncertainties, modeling mistakes, and optimality, were also included [1]. A near-optimal approach is commonly computed to decrease the runtime required of an issue in a real-world application [2]. Generally, motion planning is a challenging problem since it requires optimizing both geometry constraints and the geometric path time (such as collision avoidance and dynamic constraints). The motion-planning issue is frequently separated to decrease complications [3–6]. An increased geometry route planner generates a route for a robot in the initial phase, taking into account geometric restrictions while disregarding the dynamic system. A velocity characteristic for a predetermined path is created in the following trajectory planning and

velocity profile generation phase when each and every robot's restrictions are imposed on the preceding path. A scalar route coordinate $(\theta(t))$ maybe utilized to indicate robot location on the path because the intended path has previously been specified in this stage [7–9]. The scalar route coordinates have the advantage of reducing the state-space of the high-dimensional model of the robotic system.

Mobile robots are generally defined by the performance of robotic motions that are being employed in a variety of application fields. Holonomic mobile robots including three-wheeled Omni-directional mobile robots (TOMRs), may conduct rotational and translational motion independently from any beginning configuration, contrasting nonholonomic variance-driven mobile robots [10–12]. As a requirement for efficient controller construction, omnidirectional mobile robots are extensively investigated.

The dynamic modeling of the Omni-directional robot orthogonally is constructed [13, 14]. Since then, a model is developed wherein the robot's location is determined by reduced geometric connections [15]. A new model [16], a basic model of its friction among the floor and robot's wheels, considers the impact of sliding. In addition, generally dynamic properties of n-wheeled mobile robots with control redundancies are investigated [17]. In the global frame coordinate, more complete modeling of TOMR dynamics with motor parameters is recently introduced [18]. The time-optimal TOMR movements are discussed in this work. Several aspects of a motion, including energy usage, security, planning ease, and accuracy, should be considered as well. Nonetheless, time-optimality is a key property of a robot, according to Balkcom et al. [19].

2. Related work

Wheeled autonomous mobile robots are divided into many types. These robots are classified as non-holonomic or holonomic platforms based on their mobility restrictions. Since the inputs fed into the number of the controller is smaller rather than configurational dimensional space, nonholonomic motion does have restrictions in terms of traveling in any direction. The wheeled mobile robot is sometimes treated as a particle to make the construction of algorithms independently of the robot's mobility restrictions easier. Differential, tricycle, bicycle, automobile, omnidirectional, synchronous, and tracked vehicles are the various driving modes of wheeled mobile robots [20]. The process begins with perception as well as progress to motion control, which is the final stage before completing correct movements. Moreover, based on the wheeled autonomous mobile robot setting (outdoor or inside) or the mission, the sensor data flow might be a bit variable. The perception stage decides what information about the robot's environment is required to accomplish a behavior motion. Sensors seem to be necessary components for the mobile robot to perceive its surroundings.

[21] investigated the impact of processing as well as sensing energy usage. However this stage seems to have the potential to impact energy usage, it has received little attention. The autonomous wheeled mobile robot, for example, does not require the usage of all sensors at an identical time. It may use different sensors depending on the accuracy necessary for the perception stage as well as swap among them at appropriate moments [22]. The mapping step simulates the environment once the robot has detected its surroundings. It combines the data acquired by the sensors into a visual representation. As

a result, the AWMR's position is determined during the localization stage. Even though both phases are critical during missions as they consume very little energy. Utilizing appropriate algorithms, on the other hand, can reduce CPU demands. The steps of planning, as well as motion controlling, have a direct impact on the motion. Furthermore, to determine research gaps, the researchers divide current publications on energy in navigating phases as planning as well as motion control stages.

3. Systematic Approach

Assuming $q = (x, y, \theta)$, as the robotics state whereas the robot's center is located at the angle acquired by the line between the center approaching the very first wheel horizontally as illustrated in Figure 1. Considering the distance between the robot's center and the wheels is obtained without losing generality. Additionally assuming three wheel-speed controllers, v1, v2, as well as v3, are all in the range [-1, 1].

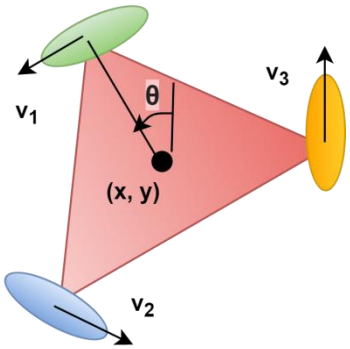

Figure 1: The robotic model.

3.1. Geometric Interpretation of the Switching Functions:

The geometric explanation of the switching functions may be found here. Assume the $\eta(x, y)$ function:

$$\eta(x, y) = k_1 y - k_2 x + k_3 \quad (1)$$

The $\eta(x, y)$ is indicated as the scaled distance between a point (x, y) as well as a line in the plane wherein, its position is defined by the parameters k_1, k_2, as well as k_3. Then, considering the line exist 'at infinity' whether $k_1^2 + k_2^2 = 0$, this line is known to be a switching line. Lets the switching line's direction is provided, hence any point (x, y) will be on the left side of the switching line when $\eta(x, y) > 0$ whereas it lies on the right side of the switching line when $\eta(x, y) < 0$.

3.1.1. Theorem 1:

Establish the rigidly connected points namely S_1, S_2, as well as S_3 with a certain distance from the robot center as well as 60◦, 180◦, and 300◦ angles with the ray from robot center to wheel 1, as shown in Figure 2. There are constants k_1, k_2, k_3, as well as a line namely the switching line for each time-optimal robot trajectory to target in order to minimize the motion time.

$$L = \{(a, b) \in R^2 : k_1 b - k_2 a + k_3 = 0\} \quad (2)$$

Therefore, the point locations such as S_1, S_2, as well as S_3 are relative to the line determines the robot motion control with the minimum time v_1, v_2, as well as v_3. In particular, for i ∈ {1, 2, 3},

$$v_i = \begin{cases} 1 \; if \; S_i \; is \; to \; the \; right \; of \; the \; switching \; line. \\ -1 \; if \; S_i \; is \; to \; the \; left \; of \; the \; switching \; line. \end{cases} \quad (3)$$

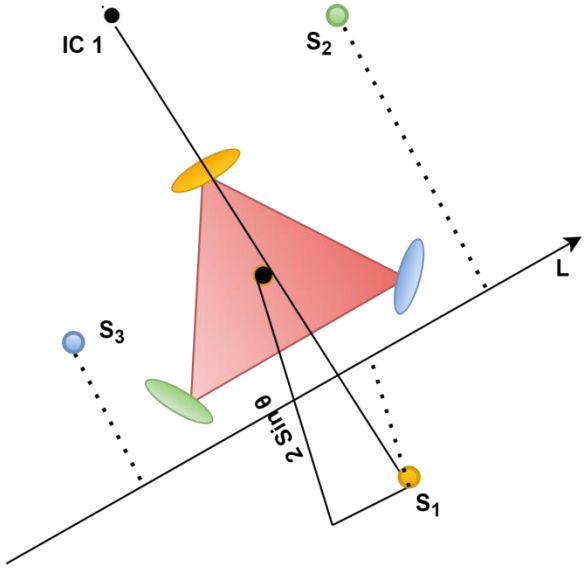

Figure 2: Geometric interpretation of switching function.

Proof:

Assuming, the coordination of S_i are (x_{S_i}, y_{S_i}). We find that $\varphi_i(x, y, \theta) = \eta(x_{S_i}, y_{S_i})$ defines the switching functions, then computing the scaling distance from the line L of point S_i.

S_1, S_2, as well as S_3 are the switching positions. The switching line location is set by the selecting constants for any time-optimum trajectory of the robot, as well as the controls at each point is determined whereas the switching function's magnitude is not determined. An instance is shown in Figure 2. S_2 and S_3 are the two switches positioned on the left side of the switching line, the associated functional switching is non-negative, and wheel 2 and wheel 3 are spinning in the opposite direction at high speed with minimum time. Wheel 1 spins at high speed in the positive direction with minimal motion time since the residual switching point (S_1) seem to be on the right side of the switching line. The time-optimal robot would pursue a circular arc with the clockwise motion as an outcome of such a control system. The center arc is at a certain distance from the robot, and then it runs along the line that connects the robot's center with wheel 1.

The control systems consider the entire maximum or lowest value, the robot rotates in location, whether all 3 switching functions possess a similar indication. The rotation center is the robot's center, which refers to as IC 0. The robot revolves in a circular arc when there are non-zero switching

functions but not all possess a similar indication. The ray linking the robot center and the wheel correlating to the minimum switching function, then the rotational center is a certain distance from the robot center. The rotational centers correlating to every wheel are referred to as IC 1, IC 2, as well as IC 3.

A combination of several switching functions remains unaffected by robot parallel translation as shown in Figure 2. While the positive constant has no impact on the switching functions, controlling does. frame on the switching line regarding the x-axis and an appropriate balancing plane, such that y represents the switching line's distance and θ ensures that regardless of sacrificing generality, the robot's tilt relative to the switching line remains constant. When using this set of coordinates, the switching functions are more efficient.

$$\varphi_1 = y - 2s_1 \quad (4)$$

$$\varphi_2 = y - 2s_2 \quad (5)$$

$$\varphi_3 = y - 2s_3 \quad (6)$$

The robot can spin in location, travel in a circular arc, move in the perpendicular direction to the line connecting two wheels, or move in the parallel direction to the line connecting two wheels. Every control is denoted using a symbol, such as $S_{i,j}, P_{\pm}, C_{\pm}, or\ D_{k\pm}$. The subscripts are determined by the switching function's particular indications. Theorem 1 explains the extremal controls in explicit geometrical terms. The controls are based on where the switching points are concerning with the switching line.

3.2. Wiggling up and down:

When the robot is at a safe distance from the switching line, all wheels spin in the same direction. A Figure 3 example is shown. The robot rotates clockwise (P-) when it is on the left side of the switching line and rotates counterclockwise (P+) when it is on the right side of the switching line.

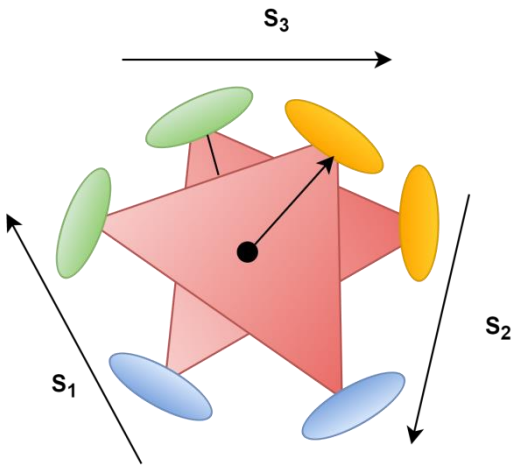

Figure 3: Spin motion control.

3.3. Circular arc:

Figure 4 depicts a counterclockwise arc about IC 2 (C_{2+}). When 2 switching points are present on the identical side of the line whereas the opposing side of the line contains a single point, in a particular direction these two wheels spin at high speed with the minimum time and in the opposing direction the remaining one wheel spins at high speed with minimum motion time. These control systems provoke the robot to implement a circular arc with a radius; then IC is proportional to the switching point which is not on the identical side whereas the remaining one point is at the arc center, and the rotational direction is determined by if the switching point is on either right or left side of the line.

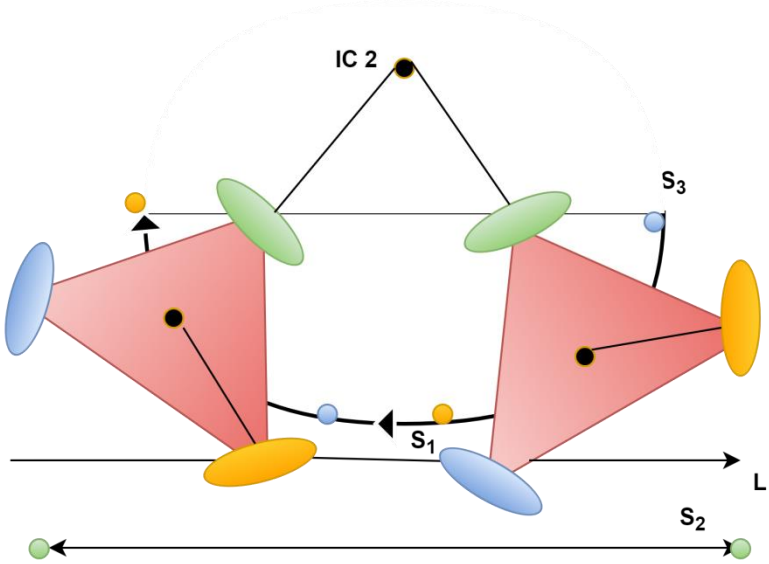

Figure 4: Circular arc motion control.

3.4. Tangent:

The switching points following circular arcs spin the robot in stationary or following a circular arc. When anyone such arcs are perpendicular to the switching line, then a solitary control is feasible at the tangential point, and the robot can translate together with the switching line for an indefinite length of time until a circular arc is resumed. Figure 5 depicts the tangential motion. A tangent trajectory motion of robot divides a one circular arc further into three parts. Single S straights, perhaps of zero duration divide those segments. As illustrated in Figure 5, the arc portions are C^{start}, C^{mid}, as well as C^{end}. In a whole C^{mid} section, the robot spins around 60◦ degrees.

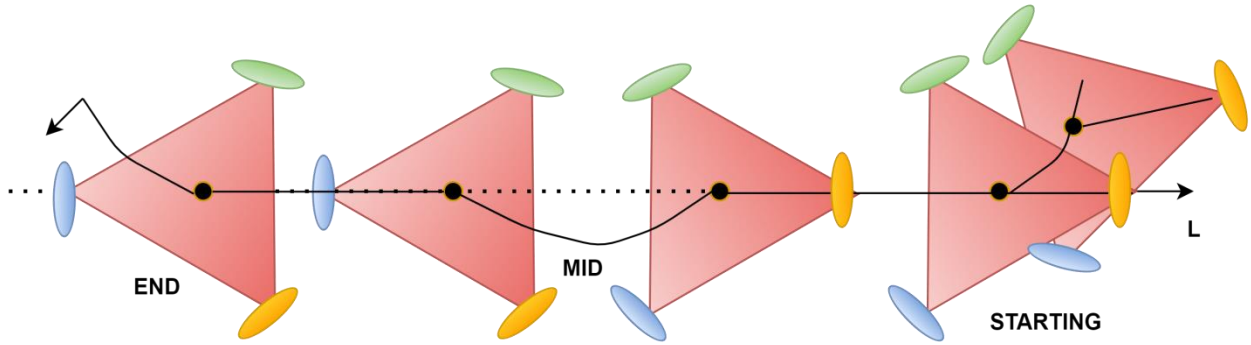

Figure 5: Tangent trajectory motion of the robot

4. Result and Discussion

Simulations backed with our theoretical findings. We demonstrate that, despite being dependent on the robot kinematics, Property 1 exhibits significant concordance with the dynamic simulation. The robot travels a straight route of five meters throughout all scenarios of motion. The experiments have a 1-millisecond resolution; they end once the error falls under 0.1 percent. In the first experiment, various instances of rotation are provided. Using the same symmetry as previously stated, the robot starting headings are picked in the range of approximately −60◦ to 60◦. The experiment demonstrates that, except for the time-optimum, enabling rotation always results in a quicker transit, confirming Property 1. If the beginning direction is ±30◦, the trajectory motion time with all the scenarios rotation is 14.4% greater than when rotation is allowed. We can also observe that if the robot heading to the target via the trajectory movement of the robot underspin, circular arc, and tangential motion and the ideal input vector is the lowest motion time under rotation is obtained.

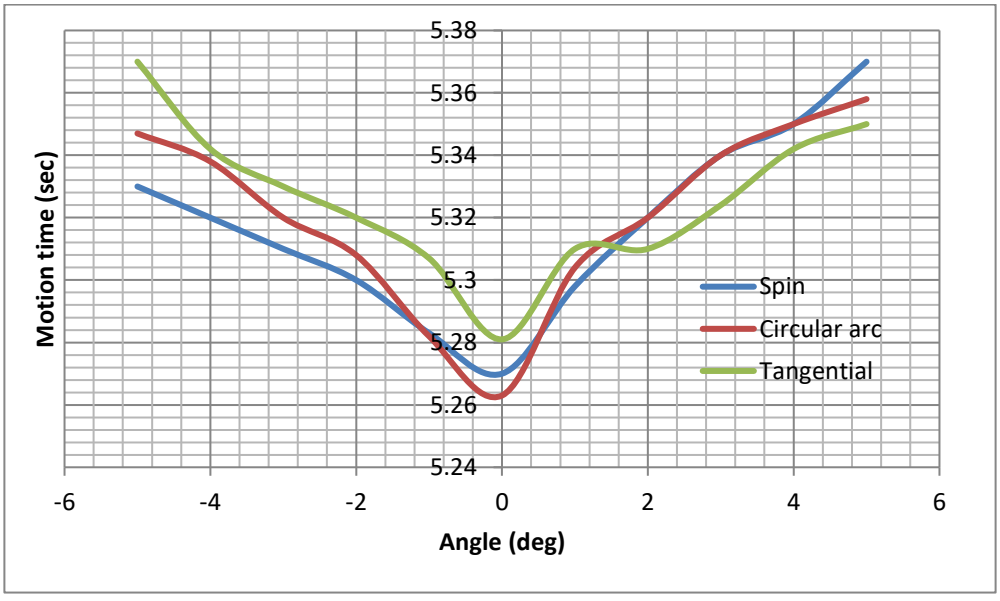

Figure 6: Spin, circular arc, and tangential motion for a robot.

Figure 6 illustrates that when the robot starting heading is not a maximum translational angle, the robot's quickest transit is obtained with the minimum motion time. The horizontal axis with the angle offset denotes the angle changed before the robot's translational movement. The indication of offset angles denotes a shift in the starting trajectory approaching (-) or away from (+) the closest maximum translational angle. Utilizing these spin, circular arc, and tangential motions for every beginning direction does result in the shortest time-optimal trajectory. In addition, the lowering edge of the 60◦ line correlates to the quickest motion when there is no perturbation and disturbance, respectively.

5. Conclusion

In this paper, with the geometric interpretation of the switching function, the challenge of producing the fastest shortest route for a robot with minimum motion time under various conditions is investigated. Thus, we think, is the initial effort at an analytical solution to this issue. For the time-optimal robotic motion, that has practical analysis of geometric interpretation of switching function under the various motion such as spin, circular arc, and tangential motion of the robot. We also observed that the minimum motion time is influenced by the robot's starting direction, which we confirmed with simulations. A robot can spin while moving. As a result, we looked into the challenge of determining the fastest shortest route if the robot could spin, circular arc, and tangential motion. The intricacy of the dynamics precludes us from finding an explicit solution to such an issue. Nonetheless, we discovered that the quickest motion of the robot with the minimum time as per theorem 1. Thus, the experimental results give the minimum time of the robot in terms of spin, circular arc, and tangential motion. This paper will pave the path for the upcoming research in this field.

REFERENCE

1. Chang, Y.-C., Chen, C.-W., and Tsao, T.-C., 2018, “Near Time-Optimal Real-Time Path Following Under Error Tolerance and System Constraints,” ASME J. Dyn. Syst., Meas., Control, 140(7), p. 071004.
2. Arab, A., Yu, K., Yi, J., and Song, D., 2016, “Motion Planning for Aggressive Autonomous Vehicle Maneuvers,” IEEE International Conference on Automation Science and Engineering (CASE), Fort Worth, TX, Aug. 21–25, pp. 221–226.
3. Suresh, P., Rajesh, K.B. and Sivasubramonia Pillai, T.V. and Jaroszewicz, Z., “Effect of annular obstruction and numerical aperture in the focal region of high NA objective lens,” Elsevier – Optics Communication, Vol – 318, 2014, pp. 137–141.
4. Barnett, E., and Gosselin, C., 2015, “Time-Optimal Trajectory Planning of Cable-Driven Parallel Mechanisms for Fully Specified Paths With g1-Discontinuities,” ASME J. Dyn. Syst., Meas., Control, 137(7), p. 071007.
5. Otte, M., and Frazzoli, E., 2016, “RRTX: Asymptotically Optimal Single-Query Sampling-Based Motion Planning with Quick Replanning,” Int. J. Rob. Res., 35(7), pp. 797–822.
6. Xidias, E. K., 2018, “Time-Optimal Trajectory Planning for Hyper-Redundant Manipulators in 3D Workspaces,” Rob. Comput.-Integr. Manuf., 50, pp. 286–298.
7. Verscheure, D., Demeulenaere, B., Swevers, J., Schutter, J. D., and Diehl, M., 2009, “Time-Optimal Path Tracking for Robots: A Convex Optimization Approach,” IEEE Trans. Autom. Control, 54(10), pp. 2318–2327.

8. Lipp, T., and Boyd, S., 2014, "Minimum-Time Speed Optimisation Over a Fixed Path," Int. J. Control, 87(6), pp. 1297–1311.
9. Shen, P., Zhang, X., and Fang, Y., 2017, "Essential Properties of Numerical Integration for Time-Optimal Path-Constrained Trajectory Planning," IEEE Rob. Autom. Lett., 2(2), pp. 888–895.
10. M. H. Khooban, A. Alfi, and D. N. M. Abadi, "Teaching-learning-based optimal interval type-2 fuzzy PID controller design: a nonholonomic wheeled mobile robots," Robotica, vol. 31, no. 7, pp. 1059–1071, 2013.
11. M. H. Khooban, "Design an intelligent proportional-derivative (PD) feedback linearization control for nonholonomic-wheeled mobile robot," Journal of Intelligent and Fuzzy Systems, vol. 26, no. 4, pp. 1833–1843, 2014.
12. K. Shojaei, A. M. Shahri, A. Tarakameh, and B. Tabibian, "Adaptive trajectory tracking control of a differential drive wheeled mobile robot," Robotica, vol. 29, no. 3, pp. 391–402, 2011.
13. K.Watanabe, Y. Shiraishi, S. G. Tzafestas, J. Tang, and T. Fukuda, "Feedback control of an omnidirectional autonomous platform for mobile service robots," Journal of Intelligent and Robotic Systems, vol. 22, no. 3-4, pp. 315–330, 1998.
14. Suresh, P., Thilagavathi. R., Gokulakrishnan, K., Rajesh, K.B. and Pillai, T.V.S., "Focusing properties of a 4Pi configuration system under the illumination of double ring shaped LG11 beam," Springer – Optical and Quantum Electronics, 1-6, 2014
15. T. Kalmar-Nagy, R. D'Andrea, and P. Ganguly, "Near-optimal ´ dynamic trajectory generation and control of an omnidirectional vehicle," Robotics and Autonomous Systems, vol. 46, no. 1, pp. 47–64, 2004.
16. R. L. Williams II, B. E. Carter, P. Gallina, and G. Rosati, "Dynamic model with slip for wheeled omnidirectional robots," IEEE Transactions on Robotics and Automation, vol. 18, no. 3, pp. 285–293, 2002.
17. Suresh, P., Mariyal, C., Rajesh, K.B. and Pillai, T.V.S., "Polarization effect of cylindrical vector beam in high numerical aperture lens Axicon systems," Elsevier – Optik, Vol. 124, 2013. pp. 1632-1636
18. K. B. Kim and B. K. Kim, "Minimum-time trajectory for three-wheeled omnidirectional mobile robots following a bounded-curvature path with a referenced heading profile," IEEE Transactions on Robotics, vol. 27, no. 4, pp. 800–808, 2011.
19. D. J. Balkcom, P. A. Kavathekar, and M. T. Mason, "Timeoptimal trajectories for an omni-directional vehicle," International Journal of Robotics Research, vol. 25, no. 10, pp. 985–999, 2006.
20. Klancar, G.; Zdesar, A.; Blazic, S.; Skrjanc, I. Wheeled Mobile Robotics: From Fundamentals Towards Autonomous Systems; Butterworth Heinemann: Oxford, UK, 2017.
21. Suresh, P., Mariyal, C., Gokulakrishnan, K., Rajesh, K.B. and Pillai, T.V.S., "Tight Focusing of Circularly Polarized Beam over high NA Lens Axicon with a Diffractive Optical Element," Elsevier – Optik, vol. 124. Issue 20, 2013. pp. 4389-4392
22. Ondrúška, P.; Gurău, C.; Marchegiani, L.; Tong, C.H.; Posner, I. Scheduled perception for energy-efficient path following. In Proceedings of the 2015 IEEE International Conference on Robotics and Automation (ICRA), Seattle, WA, USA, 26–30 May 2015; IEEE: New York, NY, USA; pp. 4799–4806.